

14th Congress of the International Society of Photogrammetry,
Hamburg 1980

Commission No. III - Working Group No. III/2

Wolfgang Mehl

Commission of the European Communities
Joint Research Centre - Ispra Establishment
I-21020 Ispra, Italy

AUTOMATIC NOISE REMOVAL AND CONTOUR MAPPING ON LOW
GRADIENT IMAGERY

Abstract

Digital imagery obtained from multispectral scanner data over water bodies generally display low gradient features. The readability of such images is improved if continuous equidensity curves are superimposed onto the imagery. A series of algorithms to be used for generating such curves on noisy data is presented. These include procedures for reducing random line offset variations, and random noise, and for generating the contour curves. The described techniques can be implemented on mini-computers with limited address space. Applications on Coastal Zone Colour Scanner data are shown.

1. BACKGROUND

In October, 1978 NASA launched the Coastal Zone Colour Scanner (CZCS) on board the Nimbus 7 satellite. The CZCS measures upwelling spectral radiances from the ocean waters in thermal and near-infrared (the latter for land recognition only) and four visible bands which are selected according to optical properties of chlorophyll, yellow substances, and suspended matter.

The design characteristics of the CZCS permit to study the feasibility of

- determining the nature and quantity of materials suspended in ocean waters, using a space-borne optical sensor,
- applying the observations to the mapping of algal biomass in biologically productive areas and of suspended sediments in coastal zones,
- detecting pollutants.

The Joint Research Centre of the European Communities participates in the Nimbus-7 CZCS experiment in collaboration with a number of national laboratories of the EC member states. The project, called EURASEP, is

described in [1].

2. PROBLEMS

Extracting maps of physical quantities (concentrations of pigments and of inorganic suspended matter) from CZCS data requires the following steps:

- 1) Calibrating the data acquired by the scanner in physical units, i. e. radiance.
- 2) Estimating the radiance which would have been measured below the surface; depending on the spectral band, 80 percent or more of the light intensity measured by the instrument is sun light scattered by air molecules or aerosols into the optical path.
- 3) Determining the concentrations of pigments or sediments.
- 4) Producing a comprehensive map output.

The modeling of the radiation transfer required for steps 2) and 3) has been discussed in [2] and [3] and shall not be considered here. Our concern will only be the use of image processing techniques not based on physical models. In particular, the following problems are studied:

- 1) Given the low response of water with respect to the total measured radiance, small interline variations of calibration are enhanced through atmospheric correction. Such calibration variations are present in initial CZCS imagery in the form of banding.
- 2) Both atmospheric correction procedures implemented at the JRC (see [2]) have shown to fail over large extensions (500 x 500 picture elements corresponding roughly to 400 x 600 km; see figures 1 and 2). Therefore a method for separating long-distance brightness changes and local brightness changes might prove useful.
- 3) Algorithms used for extracting physical quantities (sub-surface radiance, pigment concentration, etc.) compute one or more values for each picture element of the multichannel input image, i. e. their result is again an image. As the output image contains noise (which normally is even enhanced with respect to the input image) and many more grey levels than the human eye could distinguish on a visual display of the image, it is not suited for map output of numeric values. Methods for generating maps are required in which for any location the represented value can be extracted easily and with sufficient accuracy.

3. FILTERS

The introduction of some notation will facilitate the further discussion. Let \mathbb{Z} be the set of signed integers, \mathbb{R} be the set of real numbers, U a subset of $\mathbb{Z} \times \mathbb{Z}$ (the cartesian product of \mathbb{Z} with itself), and B a subset of \mathbb{R} . Then a function $I : U \rightarrow B$ is called an image on U into B . For a given $i \in \mathbb{Z}$, the restriction of I to the set of all (i, j) in U is called

the i -th line, the restriction to the set of all (j, i) in U is called the i -th image column. The restriction of I to a single element (i, j) is called a pixel.

Let U be a finite subset of $\mathbb{Z} \times \mathbb{Z}$, B a subset of \mathbb{R} , and $\mathcal{C}(U, B)$ the set of all images on U into B . Then a function $F : \mathcal{C}(U, B) \rightarrow B$ is called a filter on U into B . The product of an image I on $\mathbb{Z} \times \mathbb{Z}$ into B and a filter F on U into B in an image

$$J = IF$$

on $\mathbb{Z} \times \mathbb{Z}$ into B , can be defined as follows:

For each (i, j) in $\mathbb{Z} \times \mathbb{Z}$, the restriction of I onto the set U_{ij} of pairs (i', j') with $(i' - i, j' - j)$ in U defines an element C_{ij} of $\mathcal{C}(U, B)$, thus a value of C_{ij} and F which is the value of (i, j) under J . Note that U_{ij} is congruent to U and has the same position with respect to (i, j) which occupies U with respect to $(0, 0)$.

Example: Let U be $\{(0, 0), (0, 1)\}$, and the value KF of an image K on U be $(0, 0)K + (0, 1)K$. Then the image $J = IF$ maps (i, j) onto $(i, j)I + (i, j+1)I$.

Note that according to the definitions above, a filter is always associated with a subset of $\mathbb{Z} \times \mathbb{Z}$ and a subset of \mathbb{R} . We shall call two filters F on U into B and G on V into B isomorphic if for each image I into B , $IF = IG$. Furthermore, we shall not distinguish between filters and the isomorphism classes they belong to, and shall call the intersection of the subsets of $\mathbb{Z} \times \mathbb{Z}$ associated with all filters in an isomorphism class, the domain of the filters belonging to that class; the subset B of \mathbb{R} is called the codomain. The product FG of filters F, G on B is defined through $I(FG) = (IF)G$ for all I . If the codomain B of filters F and G is closed with respect to addition, the sum $F + G$ is defined through $(i, j)I(F + G) = (i, j)IF + (i, j)IG$ for all I .

Filters of particular interest are:

scalar filters, i. e. those with domain $\{(0, 0)\}$;

linear scalar filters, defined through $(0, 0)IF = \lambda \cdot (0, 0)I$;

translations, i. e. those with domain $\{(i, j)\}$ such that $(i, j)IF = (i, j)I$;

linear filters, i. e. those which are generated by linear scalar filters and translations through a finite number of additions and multiplications.

4. REMOVAL OF BANDING

The algorithm used for suppressing banding in scanner data over water is described briefly in [2]. It will be stated here using the notation above.

Let I be an image on a finite subset S of $\mathbb{Z} \times \mathbb{Z}$ into \mathbb{R} . The product of a filter with I is not defined; however, I can be embedded into an image I' on $\mathbb{Z} \times \mathbb{Z}$ in the following way: since S is finite, there exists an r in \mathbb{R} which is not contained in SI . Extend I to I' through: $(i, j)I' = r$ for any (i, j) which is not contained in S . Now consider the following class of filters into \mathbb{R} : let

$U_{(m,n)}$ be the set of all pairs (i, j) in $\mathbb{Z} \times \mathbb{Z}$ with $-m \leq i \leq m$, $-n \leq j \leq n$. A filter $A_{(m,n)}^r$ with domain $U_{(m,n)}$ exists which maps any image J on $U_{(m,n)}$ into the average over all $(i, j) \in U_{(m,n)}$ with $(i, j) \neq r$, or to r if there are no $(i, j) \in U_{(m,n)}$ with $(i, j) \neq r$. The banding removal algorithm on image I is equivalent to multiplying a filter $A_{(m,n)}^r = A_{(0,n)}^r + A_{(0,0)}^r$ with I' where n is larger or equal to $\max\{|i - i'| / (j, i) \in S, (j, i) \in S\}$.

Note that the extension of an image I through a value r is indeed performed in a computational representation of the image through marking all pixels within the rectangular stored image area which are to be excluded from processing with such a value. Of course, it is not necessary to extend the stored image area beyond its limits for computing the filtered image for the filter described above in a real implementation of the filter.

5. LOCAL STRUCTURE FILTERING

Another way of extending an image for multiplying it with a filter is often useful. If the image I is defined on (i, n) and (j, n) with $j > i$, but not on all (k, n) with $i < k < n$, then the image can be extended on (k, n) through interpolation:

$$(k, n)I' = (i, n)I + \frac{1}{j-i-1} ((j, n)I - (i, n)I).$$

Similarly, an image defined on (n, i) and (n, j) but not on (n, k) with k between i and j can be extended. The first extension is used for substituting bad lines (which are not considered part of the image here). If an image is to be extended to (m, n) and cannot be extended through interpolation, it can be however extended as $(m, n)I' = (i, j)I$, where (i, j) is the element in the domain of I next to (m, n) in the sense of euclidean distance or city-block distance.

On images extended through interpolation/extrapolation, a filter $A_{(m,n)}$ is defined which is equal to $A_{(m,n)}^r$ except that it does not exclude any value from averaging. The filter $A_{(m,n)}$ is a linear filter. Note that $A_{(0,0)} = A_{(0,0)}^r$.

If m and n are properly chosen, the filter $A_{(0,0)} - A_{(m,n)}$ enhances local structures by removing any large-scale non-uniformity. An example of banding removal and local structure enhancement is shown in Figs. (1) - (3). Fig. (1) shows the 443 nm channel of part of a CZCS scene (256 x 512 pixels) over the Balearic Islands in the Mediterranean Sea. Land and clouds are excluded from the image (shown in black). Fig. (2) demonstrates the substitution of bad lines through interpolation, and multiplication with $A_{(0,0)} - A_{(m,0)}^{255} + A_{(m,19)}^{255}$ (m sufficiently big). Fig. (2) actually shows already the computed water sub-surface radiance, but after a scalar filtering for matching contrast with Fig. (1), the scan-angle depending differences between the two images are not appreciable. Fig. (3) shows the effect of $A_{(0,0)} - A_{(15,31)}$ on the image of Fig. (2). Matching of

(m, n) to the size of the structures to be observed is necessary: for the presented scene, $A_0 - A_{(31, 31)}$ showed to preserve entirely the dark band in the lower part of the image which in Fig. (2) is hardly noticeable but with a contrast stretching as applied to Fig. (3) it would appear quite strongly. Smaller values for m and n preserve the borders but not the brightness distribution within the observed features. Note that $A_{(0, 0)} - A_{(m, n)}$ will not work properly at image borders if the image is extended with a constant.

6. IMAGE SMOOTHING AND CONTOUR MAPPING

Let I be a finite image on U into \mathbb{R} and C a finite subset of B . Contour mapping with C means marking the boundaries between connected subsets of U with values under I which lie between adjacent elements of C . From this somewhat informal definition it is clear that I must be "smooth" with respect to C , i. e. that reasonably large such connected subsets of U cover most of U . Obviously, image smoothing and contour mapping are related. An image resembling a contour map can for instance be generated in the following way: let K be the scalar filter defined through: $xK = r$ if x is in C , $xK = x$ otherwise, where r is not in $U \setminus I$. Let I' be an extension of I through interpolation/extrapolation. Then

$$IA_{(n, n)}K$$

with well chosen n will have contours marked with r . Examples of this type of contour mapping are shown in [3]. However, "contours" generated in this way are not necessarily curves but may degenerate to large areas for which $IA_{(n, n)}$ is constant and an element of C . This disadvantage is avoided with the filter

$$A_{(n, n)}L(A_{(0, 0)} - A_{(1, 1)})K,$$

where L is a scalar filter which maps each interval between adjacent elements of C onto a unique constant value (for instance its positional index with respect to the natural order in C), and K is the scalar filter defined through

$$xK = 0 \text{ for } x \leq 0, \quad xK = 1 \text{ for } x > 0.$$

For $A_{(n, n)}$ any other smoothing filter may be substituted. However, contour maps generated through linear smoothing filters do not preserve borders (i. e. curves along high gradients).

Two filters are presented here which preserve borders better than linear smoothing filters do. For simplicity, we have constructed the filters on domain $T = \{-1, 0, 1\} \times \{-1, 0, 1\}$.

Let t be a positive real number. Then we define the filter S_t for each $H \in \mathcal{C}(T, \mathbb{R})$: $H S_t$ is the average over all $(i, j)H$ for which

$$|(0,0)H - (i,j)H| \leq t, \text{ and}$$

$$|(0,0)H - (-i,-j)H| \leq t.$$

The filter can be generalized (as we implemented it) by using a weighted average.

Experience showed that filtering an image with filters S_t results in isolated points which are not modified by successive applications of S_t . Therefore the somewhat complementary filter $C_{t,n}$, n being a positive integer, has been constructed which (in the above terminology) takes the value $(0,0)H$ if the number of pairs (i,j) with

$$|(0,0)H - (i,j)H| \leq t \text{ and}$$

$$|(0,0)H - (-i,-j)H| \leq t \text{ and}$$

$$((0,0)H - (i,j)H)((0,0)H - (-i,-j)H) > 0$$

is less or equal to $2n$, and the average over the points satisfying the above conditions otherwise. The actually implemented filter has a slightly more flexible decision rule; in the presented examples, we gave weight 2 to the points $(i,0)$ and $(0,j)$ both for the count and the average computation.

Examples of these filters on the subimage of Fig. (3) shown in Fig. (4) are shown in Figs. (5) and (6). Fig. (5) shows

$$S_{16} \cdot C_{1,4} \cdot S_8 \cdot S_4 \cdot S_3 \cdot S_2 \cdot S_1 \text{ on (4),}$$

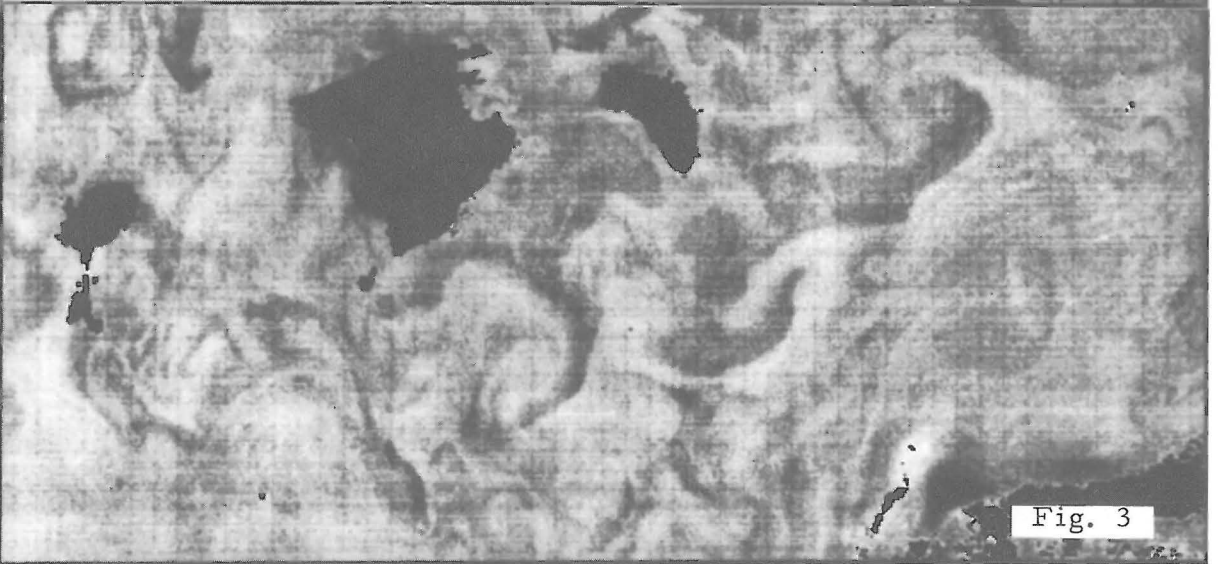
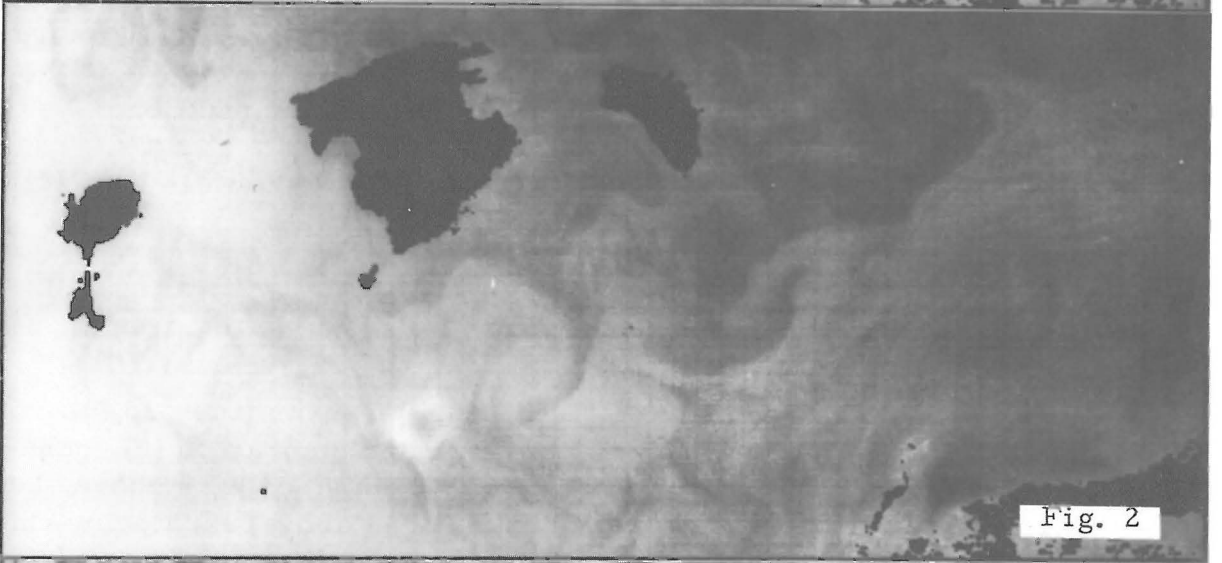
and Fig. (6) shows $C_{1,4} \cdot S_1$ on (5).

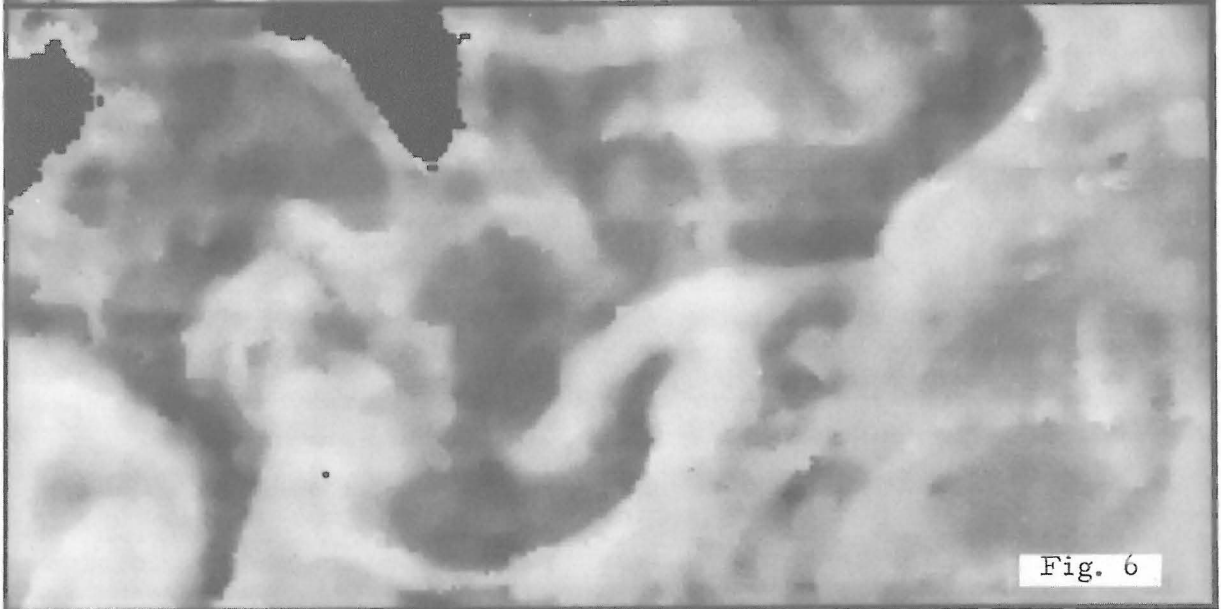
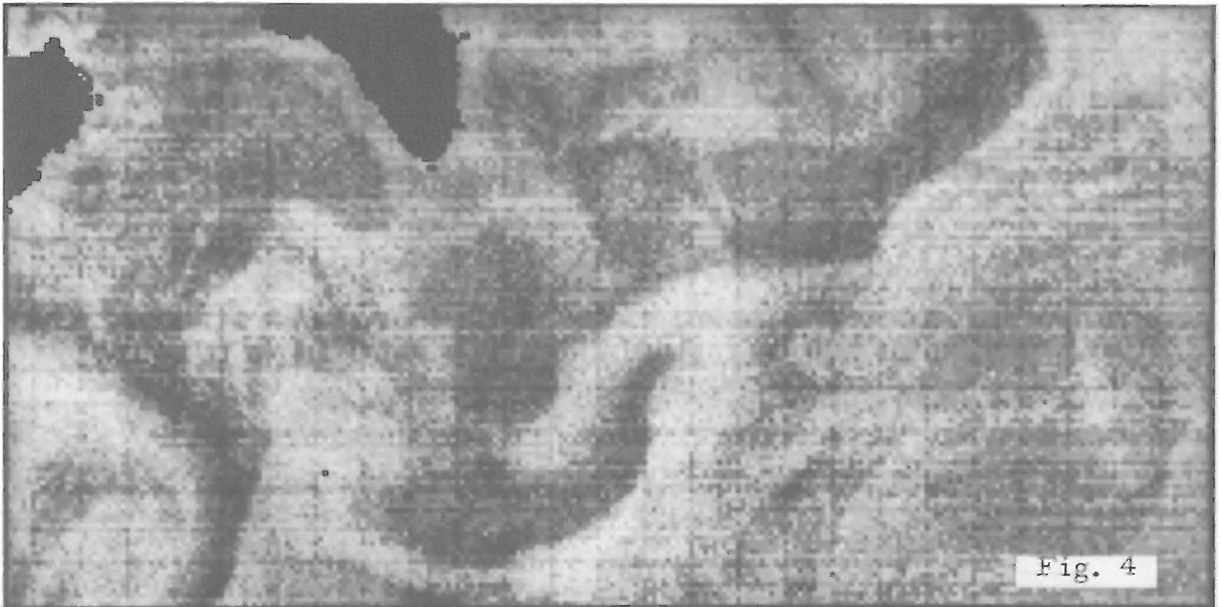
For comparison, in Fig. (7) filter $A_{(3,3)}$ is applied seven times to (4). Fig. (8) (at the bottom of the last page) shows a contour map on (6), generated not through the gradient-type filter $(A_{(0,0)} - A_{(1,1)})K$ as above, but marking (after applying a "level-slicing" filter L as above) each point which has a value larger than at least two neighbour points. Fig. (9) (center of the last page) shows the corresponding contour map on (8). It can be clearly noted that strong gradients are preserved much better through filters S_t , $C_{t,n}$ than through $A_{(3,3)}$.

REFERENCES

- [1] B. M. Sørensen, B. Sturm, W. Mehl, G. Maracci, "The First European Ocean Colour Scanner Experiment in the Southern Bight of the North Sea - EURASEP Project", 12th International Symposium on Remote Sensing of Environment, April 20-26, 1978, Manilla, Philippines.
- [2] W. Mehl, B. Sturm, W. Melchior, "Analyses of Coastal Zone Scanner Imagery over Mediterranean Coastal Waters", 14th International Symposium on Remote Sensing of Environment, April 23-30, 1980, San Jose, Costa Rica.

[3] The North Sea Ocean Colour Scanner Experiment 1977 - Final Report.
Commission of the European Communities, JRC Ispra. September
1977; edited by B. M. Sørensen.





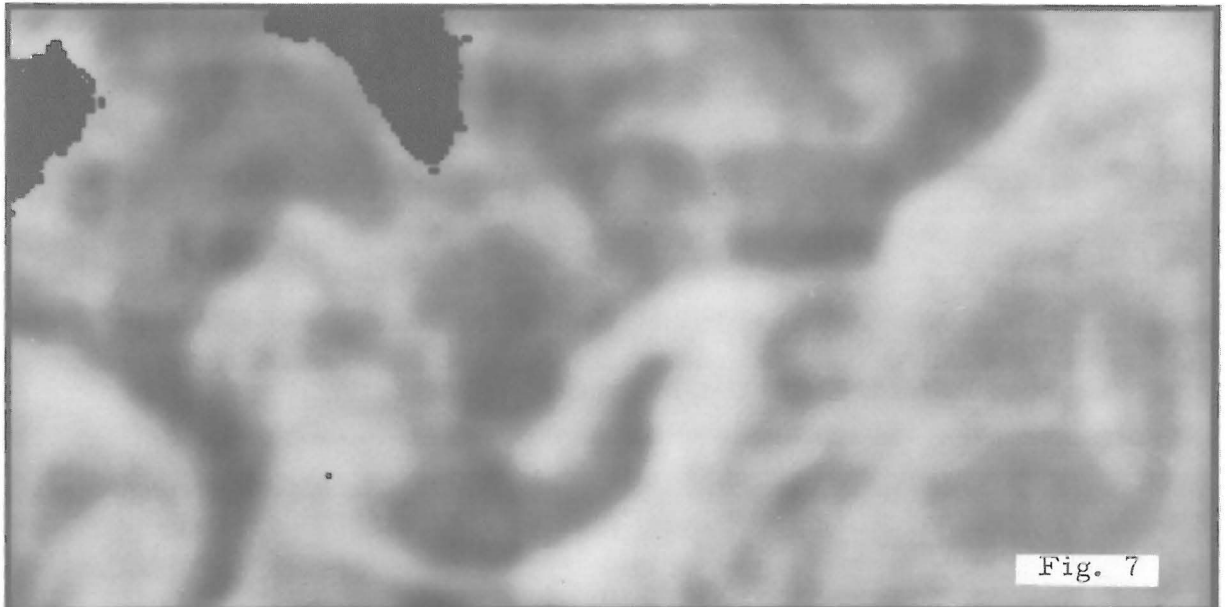


Fig. 7

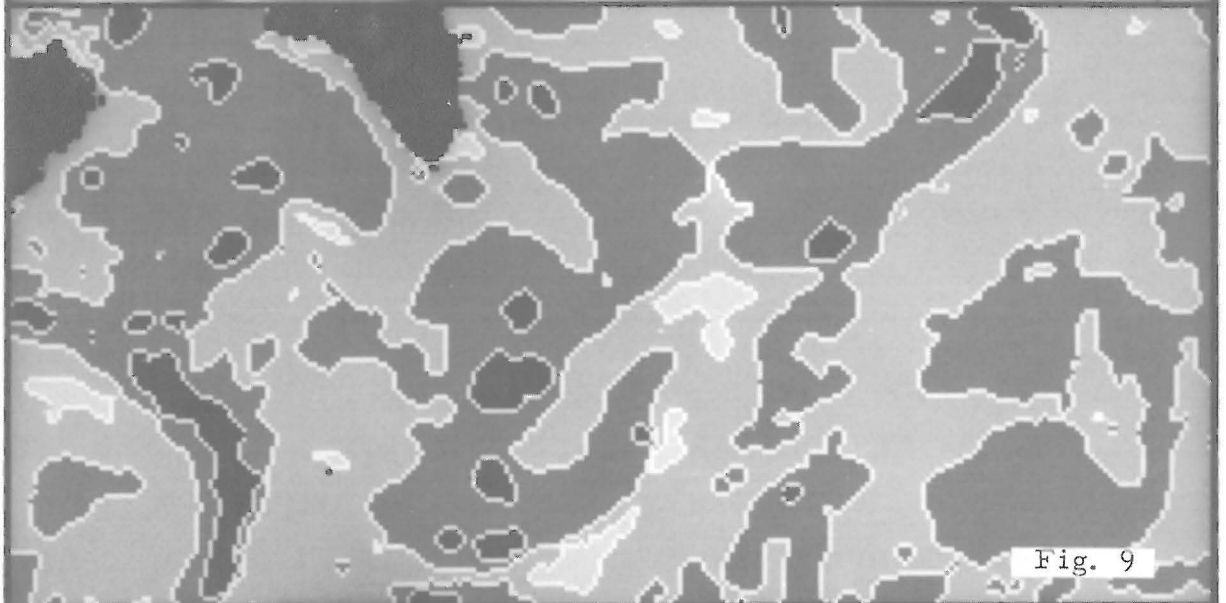


Fig. 9

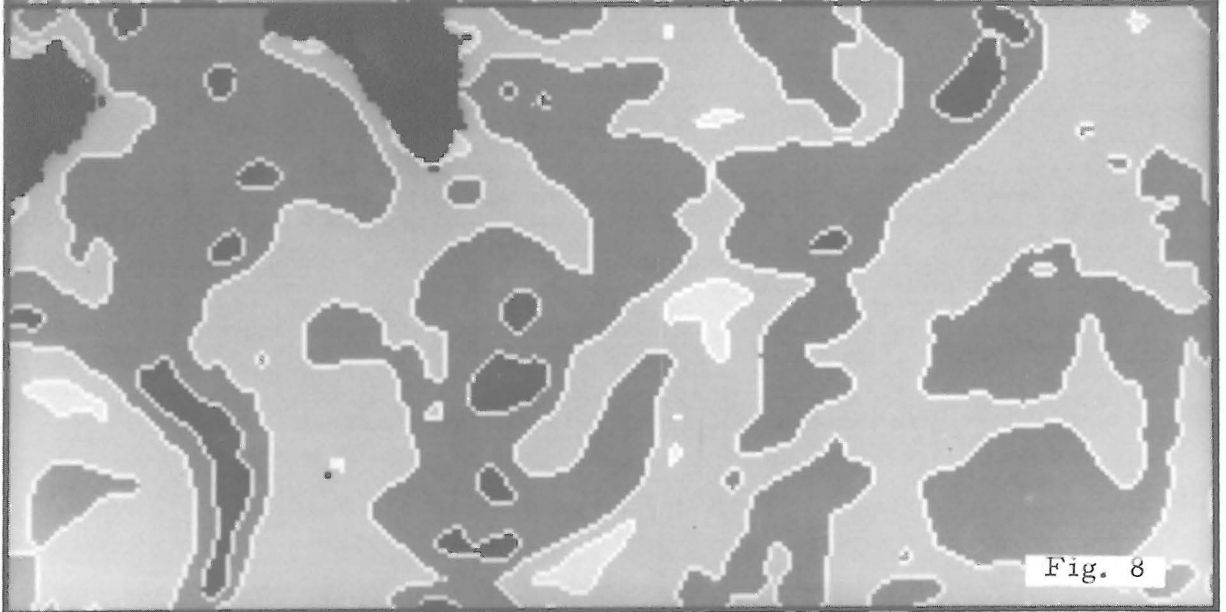


Fig. 8